Towards High-Repetition-Rate Intense Terahertz Source With Metal Wire-Based Plasma

Dongdong Zhang, Yafeng Bai, Yushan Zeng, Yingying Ding, Zhongpeng Li, Chuliang Zhou, Yuxin Leng, Liwei Song, Ye Tian, and Ruxin Li

***Abstract*—Terahertz radiation can provide unprecedented vistas in physical studies such as transient matter state control and advanced free-electron manipulation. Here, we present one feasible path towards high-repetition-rate, intense THz sources by combining the wire-based THz source on a consecutively running, wire-conveying tape design. The proof-of-principle experimental results show an upper 30 mW average THz power output under 1 kHz laser excitation, which presents the first high-repetition-rate, and most importantly, portable and application in handy THz source that is generated by solid plasmas. The generated THz pulses are characterized with a 0.3 THz center frequency and ∼0.3 THz bandwidth. We believe this tabletop laser-driven high-repetition-rate THz source will open a new door for THz and related interdisciplinary sciences.**

***Index Terms*—THz sources, THZ optics, Plasmas.**

I. Introduction

INTENSE terahertz (THz) radiation has attracted growing interest in the research area of low-frequency excitation dynamics. Since various dynamic processes including lattice vibration, molecular/atom/ion resonance excitation, and electronic spin[1]–[4] both coincide with the THz band, brand-new physical perspectives are now opened such as resonant matter control by THz transients [5], strong magnon-phonon coupling [6], and electron acceleration and manipulation [7]–[10]. Facilitating these intriguing researches requires an easily-accessible, compact, stable, and high-repetition-rate intense THz source. Nevertheless, the access of such THz sources is still challenging so far.

Conventionally, electron accelerators or free-electron lasers (FEL) underpins the demand for high-repetition, strong THz sources [11]. But the limited electron beam charge has constrained the peak electric field achieved so far. The large facility size also prohibits their wider applications. Optical rectification (OR) of femtosecond laser pulses inside nonlinear crystals or organic crystals, on the other hand, has shown to be efficient and stable for THz generation [12], [13]. Most recently, 1.4 mJ and 0.9 mJ THz pulses have been generated respectively in Lithium Niobates [14] and DSTMS [15] with an energy conversion efficiency 0.7% and 3% at 10 Hz repetition rate. However, unfortunately for these crystal-dependent sources, the presence of damage threshold and finite crystal size make further scaling of THz energy far from easy. The inevitable heat accumulation also impedes their attainable repetition rate [16]. By comparison, THz generation from laser-induced plasma involving solid, gas, and even liquid has received considerable attention owing to its damage-free nature [17] Particularly in air or liquid plasmas, where the interaction spots are constantly refreshed, high-repetition-rate (1 kHz) sources are easily obtained though being subject to a low energy conversion efficiency [18]–[22]. None of these sources currently have been an average power output over 20 mW yet. Another approach to generate high power THz radiation is based on solid plasma scheme, the record single-shot THz radiation output reaching 55 mJ [23] has been reported from the coherent transition in foil plasmas. Nevertheless, despite marking milestones in the produced energy, these studies rely on large laser systems and are generally poor at repetition rate and stability.

Consecutive exploitation of the preferred large radiation energy from solid plasmas requires the laser irradiation spot to be constantly refreshed. But this demand also poses harsh requirements on the system stability and consistency of the target. Moreover, the instability nature and complex mechanism of transition or sheath radiation further reduce the stability of the emitted THz pulses. To circumvent these difficulties, a conceptually new mechanism for THz generation has recently been proposed that depends on a femtosecond-laser-driven micrometer-diameter metal wire undulator with an energy conversion efficiency up to

Manuscript received December 14, 2021; revised December 30, 2021; accepted January 3, 2022. Date of publication January 6, 2022; date of current version January 24, 2022. This work was supported in part by the National Natural Science Foundation of China under Grants 11922412 and 11874372, in part by the Strategic Priority Research Program (B) under Grant XDB16, in part by the Shanghai Sailing Program under Grant 20YF1454900, in part by the Shanghai Commission of Science and Technology under Grant 19PJ1410500, in part by the 100 Talents Program of CAS, Youth Innovation Promotion Association of Chinese Academy of Sciences, Key Research Program of Frontier Sciences, CAS under Grant ZDBS-LY-SLH018, and in part by the Shanghai Pilot Program for Basic Research – Chinese Academy of Science, Shanghai Branch under Grant JCYJ-SHFY-2021-002. *(Corresponding authors: Ye Tian; Liwei Song; Yafeng Bai.)*

Dongdong Zhang, Yingying Ding, Zhongpeng Li, and Chuliang Zhou are with the State Key Laboratory of High Field Laser Physics and CAS Center for Excellence in Ultra-Intense Laser Science, Shanghai Institute of Optics and Fine Mechanics Chinese Academy of Sciences, Shanghai 201800, China, and also with the Center of Materials Science and Optoelectronics Engineering, University of Chinese Academy of Sciences, Beijing 100049, China (e-mail: ddzhang@siom.ac.cn; dingyy@siom.ac.cn; lizhongpeng@siom.ac.cn; chuliangzhou@siom.ac.cn).

Yafeng Bai, Yushan Zeng, Yuxin Leng, Liwei Song, Ye Tian, and Ruxin Li are with the State Key Laboratory of High Field Laser Physics and CAS Center for Excellence in Ultra-Intense Laser Science, Shanghai Institute of Optics and Fine Mechanics Chinese Academy of Sciences, Shanghai 201800, China (e-mail: baiyafeng@siom.ac.cn; yszeng@siom.ac.cn; lengyuxin@siom.ac.cn; slw@siom.ac.cn; tianye@siom.ac.cn; ruxinli@mail.siom.ac.cn).

This article has supplementary downloadable material available at https://doi.org/10.1109/JPHOT.2022.3140872, provided by the authors.

Digital Object Identifier 10.1109/JPHOT.2022.3140872

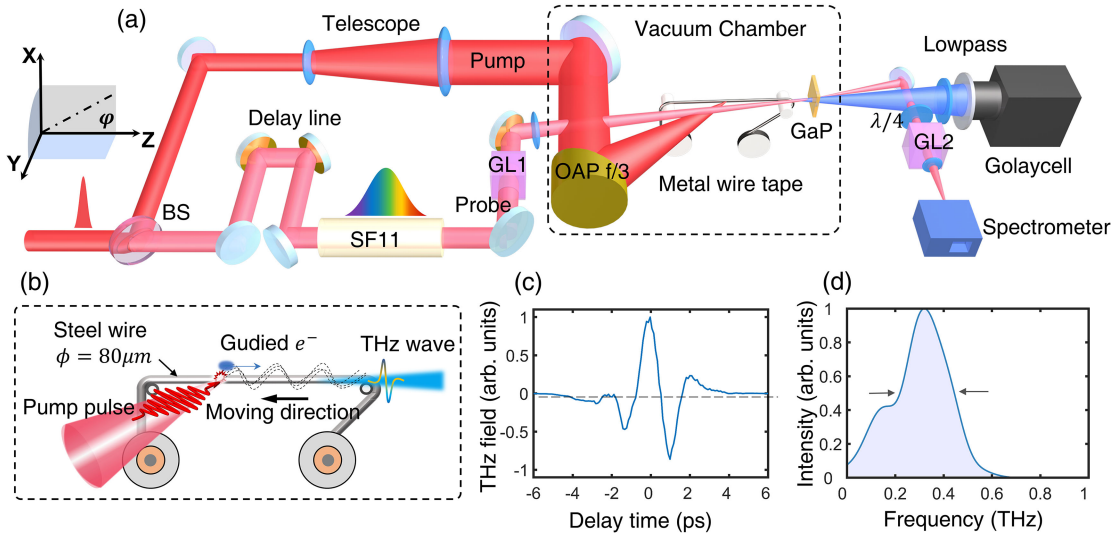

Fig. 1. Schematic illustration of the experimental setup. (a) Optical setup and the THz signal detection methods. Specifically, THz time-domain electric field is measured based on single-shot electro-optic sampling, while the THz pulse energy is measured by a Golay cell detector. The laser pulse is split into pump pulses and probe pulses with pulse energy of 3 mJ and 0.3 mJ respectively. Pump pulses are extended to 2 inches by the telescope and are then focused onto the wire by an f/3 off-axis parabolic mirror. Probe pulses are stretched from 30 fs to 8.66 ps by SF11 cylinder. A 500 μm-thick <110> GaP is placed at the tape edge for electro-optical sampling (EOS). (b) Operation diagram of wire-tape. Plasma is generated when the pump laser reaches the wire surface then, the free electrons are guided with the surface THz by the horizontal segment wire simultaneously. The THz pulse is emitted at the right end where the curvature changes. The wire moves continuously at a speed 5cm/s along the negative z-axis relative to the laser focus. (c) and (d) illustrate the typical electric field signal and spectrum of the single-shot THz in the experiment.

$\sim$1% [24]. Based on this mechanism, most recently, over 3 mJ energy THz pulse generation has been reported when the system was upscaled to an ultra-intense femtosecond driving laser system [25]. In this mechanism, an instantly excited, radially polarized strong electric field would force the laser-accelerated electrons to gyrate around the wire target, as akin to the helical undulator in an FEL. Meanwhile, the metal wire itself also serves as a natural waveguide for the THz synchrotron radiation which is collimated and guided immediately by the wire as THz surface plasmon polaritons (SPPs) and then emitted from the end of the wire [26], [27]. Consequently, emitted THz synchrotron radiation does not rely on the laser-plasma interaction directly as in the case of foil target. This new mechanism, hence, together with its compact size and high energy conversion efficiency ($\sim$1%), opens a new avenue for solid-plasma-based intense THz source [28].

In this paper, we demonstrate a tabletop, high-repetition-rate THz source based on the wire undulator mechanism with a novel wire-tape design, that can output up to 30 mW average power under 1 kHz repetition rate. Each THz pulse delivers about 30 μJ energy and $51.9kV/cm$ peak field strength, making this one of the highest average power laser driven solid plasma THz sources to date. In experiment, the consecutive THz pulse energy fluctuation is 11.7% (normalized RMS deviation), The THz pulse is characterized with $\sim$4 ps pulse duration at a center frequency of 0.3 THz and $\sim$0.3 THz (FWHM) bandwidth. Our approach opens a new path for the steady operation of the solid plasma THz sources, which paves the way for high repetition rate intense THz pulses in further applications.

II. Experiment Setup

A schematic of the experimental setup is shown in Fig. 1(a). An intense 30-femtosecond-duration laser pulse is extracted from a commercial Ti: sapphire laser (Coherent Legend Elite Duo) with a central wavelength of 800 nm and 1 kHz repetition rate. The p-polarized laser pulse is split by a 9:1 (R: T) beam splitter for pump-probe measurement. The reflected pulse (pump) is first expanded to a diameter of 2 inches and then focused by an f/3 off-axis parabolic mirror (OAP) onto the wire center, depositing about 3 mJ energy within a 5 μm (FMHW) focus spot at 45° incidence angle. As illustrated in Fig. 1(b), the wire conveying tape (WCT) constitutes the key part for our high-repetition THz source. This part is placed in a small vacuum chamber to avoid energy loss caused by air ionized plasma. Ideally, as long as the laser-irradiated spot is continuously refreshed, the wire-guided undulator would take place and radiate THz pulses with a repetition rate identical to the driving laser. In particular, the low loss and dispersion THz waveguide nature of the metal wire target [29] could offer an excellent waveguide for guiding the THz to propagate a long distance (denoted as z-axis in Fig. 1). In our setup, the emission edge of the 80μm-diameter wire is 4.5 cm away from laser-irradiation spot. THz pulses are emitted into free space at the curvature changes as shown in Fig. 2(a). According to Jefimenko equations of the transient charges will cause the waveguide THz field mode emit into free space become far-field radiation [30]. To ensure running stability of the system, a long-distance imaging microscope system is used for real-time observation and continuous monitoring of the interaction point. The THz radiation mechanism of our system is illustrated schematically in Fig. 1(b). The metal wire

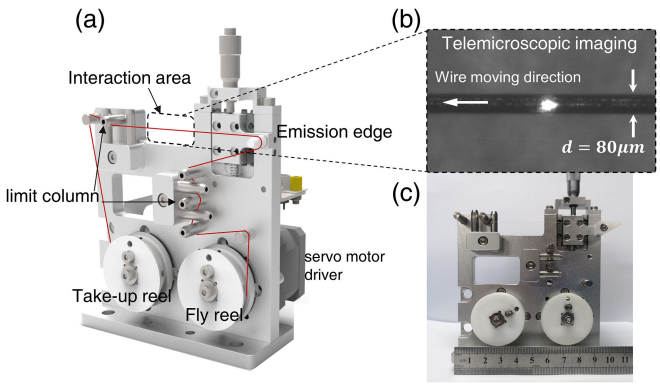

Fig. 2. (a) Function description and the 80 μm metal wire is outlined as the red solid line. (b) Real-time monitoring the spatial position of laser spots and metal wire from a telemicroscope imaging monitor. Real-time monitoring of the relative position jitter of the metal wire and the laser focus. (c) The mechanical structure of the wire conveying tape (WCT).

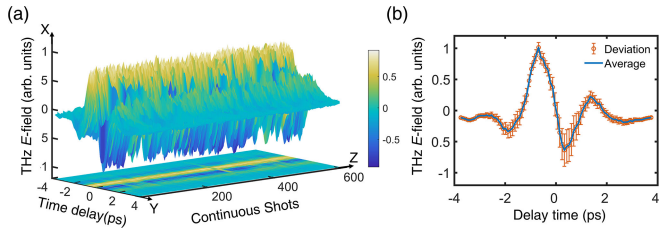

Fig. 3. (a) The THz electric field at a 20 Hz acquisition rate. The z-axis represents the continuously acquired THz pulse sequence, whereas the x-axis represents the normalized electric field and the y-axis denotes the time domain width of the pulse. (b) The deviation of the 610 shots are based on the average THz signal.

is assembled on a tape-like structure which can operate steadily under 1kHz. The transverse drift is controlled within a range of approximately $\pm 10\ \mu m$ (see Video 1).

Fig. 2 shows a mechanical diagram of the wire conveying tape structure. The module is driven by two independently controlled servo motors which could provide appropriate dragging force as well as necessary tension on the wire. The wire is made of SUS304 steel wire, a material that can withstand the large tension (that is, 520 N/mm^2) to ensure straight flowing and avoid breaking during our experiment. During the experiment, the left take-up reel collects the used wire while the right fly reel is responsible for releasing unused wire so that the laser could always interact with a fresh area. It is worth noting that, wire jitter being minimum on both vertical and horizontal directions is of utmost importance for the steady high-repetition-rate THz pulses output. To this end, we set two groups of position-limit columns at both sides of the interaction segment ("undulator" part) to guide the wire. In addition, a micrometer adjuster at the bending edge could tune the interaction segment to maintain the wire at a fine horizontal level. Thus, our configuration allows the wire to run stably and steadily along the axial direction without large lateral displacement. With one reel of 100 meters long, up to 1980 000 shots is available before replacement.

For characterization of the generated THz pulses, two independent measurements are implemented in our experiment. The THz electric field is characterized by a single-shot electro-optical sampling(EOS) measurement [31]. As shown in Fig. 1(a), the transmitted laser pulses (probe) are positively chirped from 30 fs to 8.66ps through a 50-cm-long N-SF11 glass rod, whose refractive index and group velocity dispersion are $n = 1.7859$ and $\varphi_2 = 187.50 fs^2\ /mm$ respectively at 800nm. Therefore, the full THz signal could be imprinted on the spectrum of the probe pulse by employing a 500μm thick <110> GaP crystal. Note that, the GaP is placed 1mm behind the emission edge for detecting the emitted THz in free space rather than the surface wave that propagate on wire. Hence, by analyzing the probe pulse spectral changes between the reference and THz pulse signal on GaP, the temporal THz waveform can be reconstructed using the follow equation [32],

$$E_{THz} = \frac{\lambda_0 \sin(\Delta I/I)}{2\pi n_0^3 r_{41} t\ L}$$

where $\Delta I/I = 0.3132$ is the normalized differential spectral in experiment, $\lambda_0 = 0.8\ \mu m$ is the wavelength of probe pulse, $n_0 = 3.1939$ is the refractive index of probe light in GaP, $r_{41} = 0.88\ pm/V$ is the electro-optical coefficient. The transmittance coefficient $t = 0.5275$ takes into account the overall THz intensity transmission losses introduced by the surface reflection and absorption within the crystal length $L = 500\ \mu m$. The THz pulse electric field is calculated to be $E_{THz} = 51.9\ kV/cm$.

Apart from the temporal THz waveforms characterization, THz energy measurement is also performed by a photoacoustic Golay cell detector (Tydex GC-1P) with a lowpass filter (2 mm PTFE). The THz pulse propagates from the right side of the wire and goes through the vacuum window (TPX) into the Golay cell detector. The acquisition frequency is set to 20 Hz for optimal accuracy of the Golay cell detector. The typical THz electric field waveform and spectrum are shown in Fig. 1(c, d). And the conversion factor ξ is calibrated at 20 Hz [25], [33]. Here our focus is laid on the long-time stability and high average power output of THz pulse radiation from WCT under high repetition rate excitation.

III. Results and Discussions

The results in Fig. 3 shows the experimentally obtained, continuously-recorded THz electric field waveforms and their shot-to-shot waveform drift extracted from consecutive 610 laser shots. These results give the most intuitive and unambiguous evidence of the high-repetition-rate single-cycle THz radiation generation in our experiment. By analyzing the data acquired from these continuously recorded shots, an average electric field strength of $E_{THz} = 51.9 \pm 4.6\mathrm{kV/cm}$ is detected, which though exhibits some visible deviations of the electric field strength and slight drift in the peak field in time, as shown in Fig. 3 and (see Video 2). Nevertheless, the waveform extracted from each shot remain rather similar, indicating a major progress in the exploitation of the solid-plasma-based THz sources. Specifically, in our proof-of-principle experiment, the electric field fluctuation is $\Delta E/\ E_{ave} = 8.8\%$ where ΔE is the average

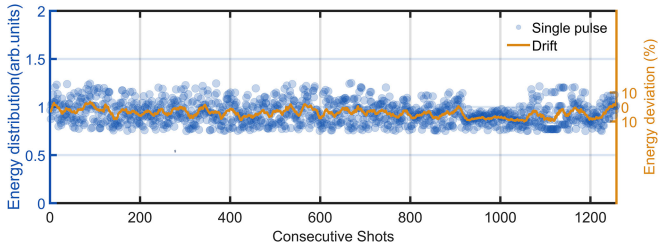

Fig. 4. THz energy fluctuation of 1250 consecutive shots was measured by Golay cell detector. Here, each blue dot represents one single THz pulse. The data are normalized based on the average value. The yellow solid line represents the energy drift over 20 shots averaged. Overall, the energy distribution shows a slow deviation at 10 percent level, which provides solid and unambiguous evidence of our high-repetition-rate wire-based source. The normalized RMS deviation (NRMSD) is 11.67%.

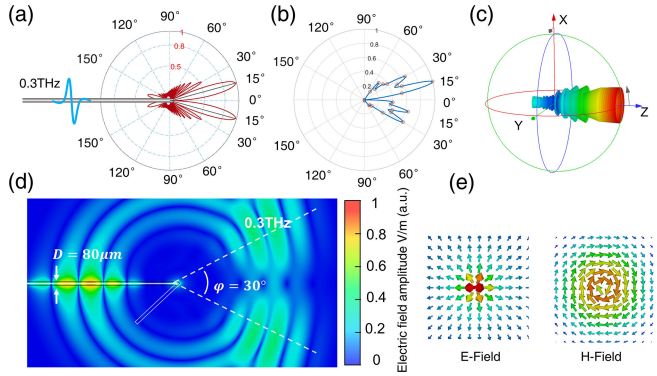

Fig. 5. Simulation of the THz emission from the WCT. (a) The far-field THz wave shows the angle distribution is a 30° narrow cone and the radial electric field and azimuthal magnetic field THz mode at the right edge. (b) Scanning far-field divergence angle in equal circumferential plane (y-z plane) with 5° as one step. (c) 3D Graphics of far-field radiation. (d) Far-field divergence angle and radiation field power in x-z plane. (e) The THz wave is free space is TM_{01}, radially polarized electric field, angularly polarized magnetic field.

fluctuation range, E_{ave} is the average electric field amplitude shown in Fig. 3(b).

To determine the emitted THz pulse energy, a Golay cell detector is placed at the emission edge of the WCT with a low-pass filter (2 mm PTFE) applied to block the infrared scattered light. In this measurement, we set the pump laser repetition rate at 20Hz so as to ensure a relatively high acquisition accuracy of the Golay cell. The results in Fig. 4 presents the acquired energy data recorded in a long-term test where 1250 shots are included. In Fig. 4, each individual dot represents one measured THz pulse energy, whereas the orange solid line represents the rolling average energy over a 1-second (i.e., 20 shots), which we defined as the pulse energy drift. On average, the energy distribution drift maintains relatively stable over the operation time and exhibits energy drifts quantified as the normalized RMS deviation (NRMSD) to be 11.67%, which is defined as $NRMSD = RMSD(\varepsilon_{deviation})/\langle\varepsilon\rangle$. Additionally, the pulse energy jitter is $\eta_W = \Delta W/W_{ave} \cong 20\%$ which is consistent with the scaling relations with field amplitude fluctuation.

Overall, 3 major factors could contribute to the THz pulse energy jitters: one related to the wire's position displacement, and the other two are related to the laser system. The first factor comes from the laser pulse energy jitter (2% in our system), which could give rise to different numbers (charges) of the electrons that radiate THz. The second factor arises from the directional stableness of the laser beam ($< \pm 3\ \mu m$ in our system). This is because the mismatch between the wire axis with the laser focus would result in the reduced power density on the wire surface, and hence declined electrons and THz power. Lastly, the position displacement of the wire during running can also exacerbate this misplacement. Among these factors, however, the wire position jitter ($< \pm 10\ \mu m$) is much bigger than the other three, considering that missing the focus spot would result in a quadratic decrease in the laser power density on the wire surface. We thus believe that improving the wire stability and steadiness while running would further elevate our current design performance, with readily applicable wire-based high-repetition-rate intense THz source just around the corner.

In addition, to better understand the emission divergence angle and the propagation mode at the right end of the WCT, an electromagnetic field transmission simulation is performed based on the experimental parameters. The THz transmission on the metal wire is simulated with aid of CST Studio Suite. As shown in Fig. 5, The wire diameter, length, and port frequency are set respectively to 80 μm, 5 cm and 0.3THz, being consistent with the experimental parameters. By using a quasi-single-cycle THz pulse, as in accordance with the experiment result, the CST can portrait the far-field radiation in the open boundary conditions of the system whose emission end has a 30° divergence angle, as illustrated in Fig. 5(a). Based on the simulation results, the THz pulses are radiated symmetrically from the emission end with a divergence angle of 30°. Experimentally, we rotate the Golay cell detector at an angle of 5° at each step on the Y-Z plane, collect the energy corresponding to different, and obtain the angular distribution of energy, the normalized divergence angle shown in Fig. 5(b) Despite the presence of energy reflection at the emission end, the result can still give a clear depiction of the radiation pattern as illustrated by the cross-section THz emitting mode in Fig. 5(d). The radial electric field and angular magnetic field indicate that the THz wave is TM01 mode as shown in Fig. 5(e). For its radial polarization feature, this THz source has the potential to be directly used in THz dielectric waveguide electron acceleration [8], [34].

IV. Conclusion

In conclusion, a high-repetition-rate, plasma-based THz has been demonstrated based on our wire conveying tape design. This tape module guarantees the stable and consistent refreshing of the target, therefore enabling the laser-plasma interaction to take place in a continuous manner. With the WCT structure and 80 μm diameter's wire applied in the experiment, we have achieved kHz repetition rate of THz radiation output based on our laser system, which to the best of our knowledge, marks the first experimental realization of high-repetition-rate plasma-based THz that promises great potential for applications. Based on our experimental results, the average power of this source could reach up to 30 mW at 1 kHz laser repetition rate, with 11.67% energy fluctuation.

This configuration could be straightforwardly extended to a 100kHz scale [35], [36] and even higher repetition-rate laser system to achieve Watt level THz average output power that is infeasible other than the enormously costly THz FEL. Moreover, a higher energy laser system that serves as the driving laser can also increase the power. With the concise, stable WCT design proposed in this letter, together with the high energy conversion efficiency $\sim$1% of the wire-based undulator mechanism, we envisage the possibility of Watt scale average power THz wave generation and numerous applications therein.

REFERENCES

[1] S. Schlauderer *et al.*, "Temporal and spectral fingerprints of ultrafast all-coherent spin switching," *Nature*, vol. 569, no. 7756, pp. 383–387, 2019.

[2] T. Kampfrath *et al.*, "Resonant and nonresonant control over matter and light by intense terahertz transients," *Nature Photon.*, vol. 7, no. 9, pp. 680–690, 2013.

[3] T. Kubacka *et al.*, "Large-amplitude spin dynamics driven by a THz pulse in resonance with an electromagnon," *Science*, vol. 343, no. 6177, pp. 1333–1336, 2014.

[4] M. Kozina *et al.*, "Terahertz-driven phonon upconversion in $SrTiO_3$," *Nature Phys.*, vol. 15, no. 4, pp. 387–392, 2019.

[5] D. Nicoletti and A. Cavalleri, "Nonlinear light–matter interaction at terahertz frequencies," *Adv. Opt. Photon.*, vol. 8, no. 3, pp. 401–464, 2016.

[6] D. L. Zhang *et al.*, "High-frequency magnetoacoustic resonance through strain-spin coupling in perpendicular magnetic multilayers," *Sci. Adv.*, vol. 6, no. 38, 2020, Art. no. abb4607.

[7] D. Zhang *et al.*, "Segmented terahertz electron accelerator and manipulator (STEAM)," *Nature Photon.*, vol. 12, no. 6, pp. 336–342, 2018.

[8] E. A. Nanni *et al.*, "Terahertz-driven linear electron acceleration," *Nature Commun.*, vol. 6, no. 1, 2015, Art. no. 8486.

[9] C. Kealhofer *et al.*, "All-optical control and metrology of electron pulses," *Science*, vol. 352, no. 6284, pp. 429–433, 2016.

[10] C. Zhou *et al.*, "Direct mapping of attosecond electron dynamics," *Nature Photon.*, vol. 15, no. 3, pp. 216–221, 2021.

[11] G. L. Carr *et al.*, "High-power terahertz radiation from relativistic electrons," *Nature*, vol. 420, no. 6912, pp. 153–156, 2002.

[12] J. Hebling *et al.*, "Tunable THz pulse generation by optical rectification of ultrashort laser pulses with tilted pulse fronts," *Appl. Phys. B*, vol. 78, no. 5, pp. 593–599, 2004.

[13] C. Ruchert *et al.*, "Scaling submillimeter single-cycle transients toward megavolts per centimeter field strength via optical rectification in the organic crystal OH1," *Opt. Lett.*, vol. 37, no. 5, pp. 899–901, 2012.

[14] B. Zhang *et al.*, "1.4-mJ High energy terahertz radiation from Lithium Niobates," *Laser Photon. Rev.*, vol. 15, 2021, Art. no. 2000295, doi: 10.1002/lpor.202000295.

[15] C. Vicario *et al.*, "Generation of 0.9-mJ THz pulses in DSTMS pumped by a $Cr:Mg_2SiO_4$ laser," *Opt. Lett.*, vol. 39, no. 23, pp. 6632–6635, 2014.

[16] L. Palfalvi *et al.*, "Nonlinear refraction and absorption of Mg doped stoichiometric and congruent $LiNbO_3$," *J. Appl. Phys.*, vol. 95, no. 3, pp. 902–908, 2004.

[17] J. A. Fulop *et al.*, "Laser-driven strong-field terahertz sources," *Adv. Opt. Mater.*, vol. 8, no. 3, 2020, Art. no. 25.

[18] K. Y. Kim *et al.*, "Coherent control of terahertz supercontinuum generation in ultrafast laser–gas interactions," *Nature Photon.*, vol. 2, no. 10, pp. 605–609, 2008.

[19] Y. S. You *et al.*, "Off-axis phase-matched terahertz emission from two-color laser-induced plasma filaments," *Phys. Rev. Lett.*, vol. 109, no. 18, 2012, Art. no. 183902.

[20] L. L. Zhang *et al.*, "Strong terahertz radiation from a liquid-water line," *Phys. Rev. Appl.*, vol. 12, no. 1, 2019, Art. no. 014005.

[21] Y. E *et al.*, "Flowing cryogenic liquid target for terahertz wave generation," *AIP Adv.*, vol. 10, no. 10, 2020, Art. no. 105119.

[22] Y. Cao *et al.*, "Broadband terahertz wave emission from liquid metal," *Appl. Phys. Lett.*, vol. 117, no. 4, 2020, Art. no. 041107.

[23] G. Q. Liao *et al.*, "Multimillijoule coherent terahertz bursts from picosecond laser-irradiated metal foils," *Proc. Nat. Acad. Sci. USA*, vol. 116, no. 10, pp. 3994–3999, 2019.

[24] Y. Tian *et al.*, "Femtosecond-laser-driven wire-guided helical undulator for intense terahertz radiation," *Nature Photon.*, vol. 11, no. 4, pp. 242–246, 2017.

[25] Y. Zeng *et al.*, "Guiding and emission of milijoule single-cycle THz pulse from laser-driven wire-like targets," *Opt. Exp.*, vol. 28, no. 10, pp. 15258–15267, 2020.

[26] W. P. E. M. op 't Root *et al.*, "Single-cycle surface plasmon polaritons on a bare metal wire excited by relativistic electrons," *Nature Commun.*, vol. 7, no. 1, 2016, Art. no. 13769.

[27] P. W. Smorenburg *et al.*, "Direct generation of terahertz surface plasmon polaritons on a wire using electron bunches," *Phys. Rev. B*, vol. 78, no. 11, 2008, Art. no. 115415.

[28] K. Nakajima, "Novel efficient THz undulator using a laser-driven wire," *Light Sci. Appl.*, vol. 6, no. 5, 2017, Art. no. e17063.

[29] K. Wang and D. M. Mittleman, "Metal wires for terahertz wave guiding," *Nature*, vol. 432, no. 7015, pp. 376–379, 2004.

[30] E. K. Miller *et al.*, "An integro-differential equation technique for the time-domain analysis of thin wire structures. I. The numerical method," *J. Comput. Phys.*, vol. 12, no. 1, pp. 24–48, 1973.

[31] Z. Jiang and X. C. Zhang, "Electro-optic measurement of THz field pulses with a chirped optical beam," *Appl. Phys. Lett.*, vol. 72, no. 16, pp. 1945–1947, 1998.

[32] C. Vicario *et al.*, "Laser-driven generation of intense single-cycle THz field," in *Proc. SPIE*, vol. 8261, 2012, pp. 227–233.

[33] Y. Wang *et al.*, "Calibration of a thermal detector for pulse energy measurement of terahertz radiation," *Opt. Lett.*, vol. 37, no. 21, pp. 4395–4397, 2012.

[34] H. Xu *et al.*, "Cascaded high-gradient terahertz-driven acceleration of relativistic electron beams," *Nature Photon.*, vol. 15, no. 6, pp. 426–430, 2021.

[35] S. Hädrich *et al.*, "3.2-mJ sub-10-fs pulses at 100 kHz," in *Proc. Laser Congr.*, 2019, paper. ATu6A.2, doi: 10.1364/ASSL.2019.ATu6A.2.

[36] S. Kühn *et al.*, "The ELI-ALPS facility: The next generation of attosecond sources," *J. Phys. B Atom. Mol. Opt.*, vol. 50, no. 13, 2017, Art. no. 132002.